

Constraining Dark Energy with Clusters: Complementarity with Other Probes

Carlos Cunha,¹ Dragan Huterer,¹ and Joshua A. Frieman²

¹*Department of Physics, University of Michigan, 450 Church St, Ann Arbor, MI 48109-1040*

²*Center for Particle Astrophysics, Fermi National Accelerator Laboratory, P. O. Box 500, Batavia, IL 60510;
Kavli Institute for Cosmological Physics, The University of Chicago, 5640 S. Ellis Ave., Chicago, IL 60637*

(Dated: August 8, 2021)

The Figure of Merit Science Working Group (FoMSWG) recently forecast the constraints on dark energy that will be achieved prior to the Joint Dark Energy Mission (JDEM) by ground-based experiments that exploit baryon acoustic oscillations, type Ia supernovae, and weak gravitational lensing. We show that cluster counts from on-going and near-future surveys should provide robust, complementary dark energy constraints. In particular, we find that optimally combined optical and Sunyaev-Zel’dovich effect cluster surveys should improve the Dark Energy Task Force (DETF) figure of merit for pre-JDEM projects by a factor of two even without prior knowledge of the nuisance parameters in the cluster mass-observable relation. Comparable improvements are achieved in the forecast precision of parameters specifying the principal component description of the dark energy equation of state parameter as well as in the growth index γ . These results indicate that cluster counts can play an important complementary role in constraining dark energy and modified gravity even if the associated systematic errors are not strongly controlled.

I. INTRODUCTION

Counts of galaxy clusters are a potentially very powerful technique to probe dark energy and the accelerating universe (e.g. [1, 2, 3, 4, 5, 6, 7, 8, 9]). The idea is an old one: count clusters as a function of redshift (and, potentially, mass), and compare to theoretical prediction which can be obtained either analytically or numerically. Recently, Rozo et al. [10] have obtained very interesting constraints on σ_8 from Sloan Digital Sky Survey (SDSS) cluster samples using the relation between mass and optical richness (the number of red-sequence galaxies in the cluster above a luminosity threshold). This follows recent dark energy constraints using optical [11] and X-ray observations of clusters [12, 13, 14].

In this paper we calculate the potential of cluster counts to improve combined constraints from the other three major probes of dark energy: baryon acoustic oscillations (BAO), type Ia supernovae (SNIa) and weak gravitational lensing (WL). We are motivated by the recently released report of the Figure of Merit Science Working Group (FoMSWG; [15]) that studied and recommended parametrizations and statistics best suited to addressing the power of cosmological probes to measure properties of dark energy. While the FoMSWG report was mainly aimed at figures of merit to be used in the upcoming competition for the Joint Dark Energy Mission (JDEM) space telescope, the applicability of its results and recommendations is general.

We address quantitatively how ongoing and upcoming cluster surveys, in particular the South Pole Telescope (SPT, [16]) and the Dark Energy Survey (DES, [17]), can strengthen the combined “pre-JDEM” constraints on dark energy considered in the FoMSWG report — that is, combined constraints expected around the year 2016. To model cluster counts, we utilize recent results from Cunha [18] which optimally combine future optical and Sunyaev-Zel’dovich (SZ) observations of clusters to esti-

mate the constraints on dark energy.

II. INFORMATION FROM CLUSTER COUNTS AND CLUSTERING

The subject of deriving cosmological constraints from cluster number counts and clustering of clusters has been treated extensively in the literature (see e.g. [18, 19, 20, 21, 22]). In this work we use cross-calibration for two observable proxies for mass: Sunyaev-Zel’dovich flux (henceforth SZ), and optical observations — which identify clusters via their galaxy members — (henceforth OPT). While we focus on optical and SZ surveys, our results are applicable to combinations of any cluster detection techniques. In particular, planned X-ray surveys such as eRosita [23], WFXT [24], and IXO [25] will have mass sensitivity competitive with, and complementary to, the SZ and optical surveys.

Our approach closely follows that in [18] and we refer the reader to that publication for basic details. In brief, cluster counts in a bin of the observables are calculated by integrating the mass function dn/dM over mass, volume, and the observable proxy in the appropriate range. We adopt the Jenkins mass function in this work, though results are weakly dependent on this choice. Clustering is given by the sample covariance of the mean counts in different redshift bins. The contribution of clustering to the constraints is very small when cross-calibration is used [18]. We allow for scatter in both the relation between mass and the observable proxy, and the relation between true and estimated photometric redshifts. Results from both simulations (e.g. [26, 27]) and observations (e.g. [28, 29, 30]) suggest that the mass-observable relations can be parametrized in simple forms with log-normal scatter of the mass-observable about the mean relation. Other works (see e.g. [31]) suggest that the distribution of galaxies in halos may be more complicated.

We assume lognormal scatter for the mass-observable relation as well as for the photometric redshift errors. We have neglected any theoretical uncertainties in the mass function, galaxy bias, and photometric redshifts, all of which must be independently known to a few percent so as not to affect cosmological constraints [21, 32].

We fix the photo- z scatter to $\sigma_z = 0.02$, the expected overall scatter of cluster photo- z 's in the Dark Energy Survey [17]. Our “theorist’s observable” quantity, which we feed into the Fisher matrix formalism to obtain constraints on cosmological parameters, is the covariance of the counts — defined as the sample covariance plus the shot noise variance — in different redshift bins.

We adopt the same surveys and parametrizations described in [18], namely, an SZ and an OPT survey on the same 4000 sq. deg. patch of sky.

Let M_{obs} be the observable proxy for mass (from either SZ or OPT survey). For the SZ survey, we define the M_{obs} threshold for detection to be $M^{\text{th}} = 10^{14.2} h^{-1} M_{\odot}$, complete up to $z = 2$, based on the projected sensitivity of the South Pole Telescope. We parametrize the mass bias (the difference between the true mass and SZ M_{obs}), and the variance in the mass-observable relation, respectively as

$$\ln M^{\text{bias}}(z) = \ln M_0^{\text{bias}} + a_1 \ln(1+z) \quad (1)$$

$$\sigma_{\ln M}^2(z) = \sigma_0^2 + \sum_{i=1}^3 b_i z^i \quad (2)$$

Fiducial mass values of all nuisance parameters are zero, except for the scatter which is set to $\sigma_0 = 0.25$ in the fiducial model. Our choice of scatter is somewhat conservative given recent studies which suggest that $\sigma_0 < 0.2$ (see e.g. [33]). However, hydrodynamics simulations by [34] find a scatter of (+32%, -16%) about the median for clusters of $M \sim 3.0 \times 10^{14} M_{\odot}$, which matches our choice. In total, there are six nuisance parameters for the mass bias and scatter ($\ln M_0^{\text{bias}}$, a_1 , σ_0^2 , b_i).

For the optical survey the mass threshold of the observable is set to $M^{\text{th}} = 10^{13.5} h^{-1} M_{\odot}$ and the redshift limit is $z = 1$, corresponding to the projected sensitivity of the Dark Energy Survey. Different studies suggest a wide range of scatter for optical observables, ranging from a constant $\sigma_{\ln M} = 0.5$ [22] to a mass-dependent scatter in the range $0.75 < \sigma_{\ln M} < 1.2$ [35]. Using weak lensing and X-ray analysis of MaxBCG selected optical clusters, Ref. [36] estimated a lognormal scatter of ~ 0.45 for $P(M|M_{\text{obs}})$, where M was determined using weak lensing and M_{obs} was an optical richness estimate. We choose a fiducial mass scatter of $\sigma_{\ln M} = 0.5$ and allow

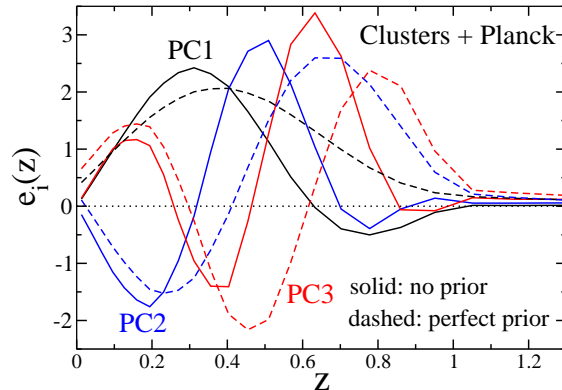


FIG. 1: First three principal components for the OPT+SZ cluster survey with Planck priors. Solid lines refer to the case with no prior on the 16 nuisance parameters, while the dashed lines correspond to the case of perfectly known nuisance parameters.

for a cubic evolution in redshift and mass:

$$\ln M^{\text{bias}}(M_{\text{obs}}, z) = \ln M_0^{\text{bias}} + a_1 \ln(1+z) + a_2 (\ln M_{\text{obs}} - \ln M_{\text{pivot}}) \quad (3)$$

$$\sigma_{\ln M}^2(M_{\text{obs}}, z) = \sigma_0^2 + \sum_{i=1}^3 b_i z^i + \sum_{i=1}^3 c_i (\ln M_{\text{obs}} - \ln M_{\text{pivot}})^i \quad (4)$$

We set $M_{\text{pivot}} = 10^{15} h^{-1} M_{\odot}$. In all, we have 10 nuisance parameters for the optical mass errors ($\ln M_0^{\text{bias}}$, a_1 , a_2 , σ_0^2 , b_i , c_i).

There are few, if any, constraints on the number of parameters necessary to realistically describe the evolution of the variance and bias with mass. Ref. [20] shows that a cubic evolution of the mass-scatter with redshift captures most of the residual uncertainty when the redshift evolution is completely free (as assumed in the Dark Energy Task Force (DETF) report [37]). Note too that we employ more nuisance parameters to describe the optical survey than the SZ survey because the former is expected to have a more complicated selection function. For the cross-calibration analysis, we assume the correlation coefficient between optical and SZ scatter ρ , defined in [18], to be fixed to zero; the same paper shows that the cross-calibration results are insensitive to the value of ρ for $\rho \in [-1, 0.6]$.

In total, we use 6+10=16 nuisance parameters to describe the systematics of the combined OPT+SZ cluster survey. While generous, this parametrization assumes a lognormal distribution of the mass-observable relation that may fail for low-masses. We have also implicitly assumed that selection effects can be described by the bias and scatter of the mass-observable relation. By the

year 2016, we expect significant progress in simulations of cluster surveys that will allow us to better parametrize the cluster selection errors.

III. COMPLEMENTARY PROBES AND FIGURES OF MERIT

To model the power of complementary probes of dark energy, we adopt the pre-JDEM information (that is, combined information projected around year 2016) based on estimates of the Figure of Merit Science Working Group [15]. These estimates include information from BAO, SNIa, WL and the Planck CMB satellite. We use these probes in combination, without or with clusters. Note that systematic errors have been included in all of these methods (see Ref. [15]).

The FoMSWG figures of merit are described in the FoMSWG paper [15] and we review them here very briefly. There are a total of 45 cosmological parameters, 36 of which describe the equation of state $w(z)$ while the others are mostly standard cosmological parameters (plus a couple of nuisance ones that have not been explicitly marginalized over). One figure-of-merit is the area in the w_0 - w_a plane [37, 38], where $w(z) = w_0 + w_a(1 - a) = w_p + w_a(a_p - a)$ and where w_p and a_p are the ‘‘pivot’’ parameter and the scale factor; we adopt $\text{FoM} \equiv 1/(\sigma(w_p) \times \sigma(w_a))$. The growth of density perturbations is described by a single parameter, the growth index γ , which is a free parameter in the fitting function for the linear growth of perturbations [39]. The figure-of-merit in the growth index is simply its inverse marginalized error, $\gamma\text{FoM} \equiv 1/\sigma(\gamma)$.

A much richer (and less prone to biases) description of the equation of state is achieved through computing the principal components (PCs) of dark energy [40], $e_i(z)$

$$1 + w(a) = \sum_{i=0}^{35} \alpha_i e_i(a), \quad (5)$$

where α_i are coefficients, and $e_i(a)$ are the eigenvectors (see [15] for details). The associated figure of merit consists of presenting the shapes $e_i(z)$ in redshift and computing the associated accuracies $\sigma(\alpha_i)$ with which the coefficients can be measured [15].

Combining the different cosmological probes is achieved by adding their associated Fisher matrices. We add the 45×45 Fisher matrix for clusters (marginalized over the mass nuisance parameters) to the combined BAO+SNIa+WL+Planck Fisher matrix and report the improvement in the figures of merit and accuracies in the PCs as well as shapes of the new PCs.

IV. RESULTS

Our baseline is the combined pre-JDEM BAO+SNIa+WL+Planck case from the FoMSWG

report. The baseline uncertainties in various dark energy parameters, after marginalization over all nuisance and cosmological parameters, are $\sigma(w_0) = 0.10$, $\sigma(w_a) = 0.31$, $\sigma(w_p) = 0.028$ ($z_p = 0.40$), $\text{FoM} = 116$, and $\sigma(\gamma) = 0.21$ ($\gamma\text{FoM} = 4.8$). These constraints are dominated by BAO+Planck which alone yield $\sigma(w_0) = 0.15$, $\sigma(w_a) = 0.44$, $\sigma(w_p) = 0.037$, $\text{FoM} = 61$. In comparison, WL+Planck and SNIa+Planck yield $\text{FoM} = 9.8$ and 0.42 , respectively.

We first consider the cluster information alone, with only a Planck prior adopted from [15]. The constraints in this case, assuming flat external priors on cluster nuisance parameters, are $\sigma(w_0) = 0.10$, $\sigma(w_a) = 0.41$, $\sigma(w_p) = 0.036$ ($z_p = 0.28$), $\text{FoM} = 66$, and $\sigma(\gamma) = 0.17$ ($\gamma\text{FoM} = 6.0$). These constraints are comparable (and complementary) to the BAO+Planck constraints. Fig. 1 shows the first three principal components for the combined (OPT+SZ) cluster survey combined with Planck. Two cases are shown: completely unknown and perfectly known nuisance parameters. In the first case, the first principal component peaks at $z \sim 0.3$, which is not surprising given that most clusters are at $z \lesssim 1$: while this peak sensitivity is at lower redshifts than that for BAO surveys, it is at slightly larger z than the peak for SNIa.

As seen in Fig. 1, adding priors to nuisance parameters moves the cluster PC weights to higher z . This is easy to understand: freedom in the nuisance parameters has progressively more deleterious effects as redshift increases, as can be deduced from Eqs. (1)-(4). Thus, priors on the nuisance parameters restore the ability of the survey to probe higher redshifts, and push the principal components to higher z .

Next, we combine the cluster information with BAO+SNIa+WL+Planck. The amount of information that clusters contribute is a strong function of the systematics assumed, in our case, a function of the *external priors* on the nuisance parameters. We find that clusters provide very significant improvement in the figures of merit even with uninformative (flat) priors on the cluster nuisance parameters. The new clusters+SNIa+WL+BAO+Planck figure of merit is 206, which is nearly a factor of two better than BAO+SNIa+WL+Planck alone. The pivot error is $\sigma(w_p) = 0.022$ ($z_p = 0.41$) which is $\sim 25\%$ better. Constraints on w_0 and w_a improve by about 50% each, since with clusters $\sigma(w_0) = 0.065$ and $\sigma(w_a) = 0.214$. Constraints on growth improve by more than a factor of 2, with $\sigma(\gamma) = 0.099$ ($\gamma\text{FoM} = 10$). The main effect of including clusters is to provide significant additional information on the growth of density perturbations. Of the complementary techniques we consider, only weak lensing probes the growth, but our fiducial cluster model gives (slightly) stronger constraints on growth than the pre-JDEM combination of BAO+SNIa+WL+Planck.

The left panel of Fig. 2 shows the best-determined three principal components for the fiducial pre-JDEM survey adopted from [15] when clusters are added, i.e. clusters+SNIa+WL+BAO+Planck. For the cluster sur-

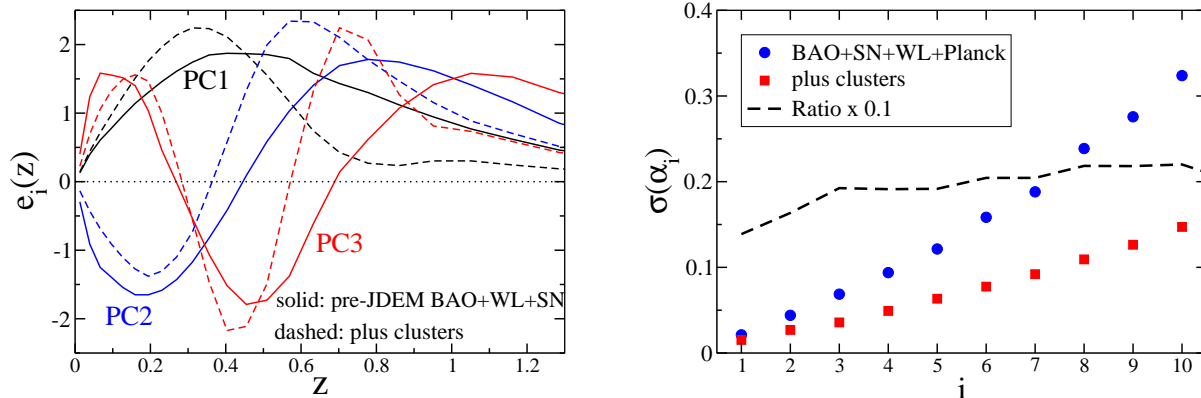


FIG. 2: Left panel: First three principal components for the SNIa+BAO+WL+Planck pre-JDEM combination alone (solid curves) and for the same combination with the addition of clusters (dashed curves). For the latter we assume OPT+SZ cluster survey with flat (i.e. uninformative) external priors on nuisance parameters. Right panel: Uncertainty in eigencoeficients of $w(a)$, $\sigma(\alpha_i)$, for the SNIa+BAO+WL+Planck pre-JDEM combination alone (circular points), and for the same combination with the addition of clusters (square points). We also show the ratio of the improvement in each eigencoeficient when clusters are added (dashed line - scaled down by a factor of 10 for clarity).

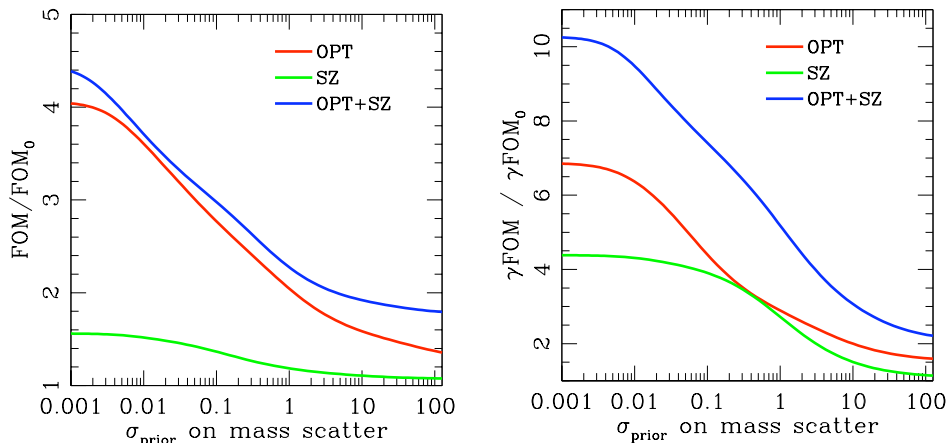


FIG. 3: Improvement in the figures of merit relative to the pre-JDEM combination (BAO+SNIa+WL+Planck) when cluster information is added. In both panels we add a uniformly increasing prior on the nuisance parameters as explained in the text, and show (on the x-axis) the effective resulting prior on the scatter in mass $\sigma_{\ln M}(M, z)$, that is, the (square root of the) left-hand sides of Eqs. (2) or (4) that correspond to the prior values of the nuisance parameters on the right-hand sides at $z = 1.0$ and $M = 10^{15} h^{-1} M_{\odot}$. For the OPT+SZ case, the uncertainty in the optical scatter is shown on the x-axis. The left panel shows the improvements in the (DETF) FoM, while the right panel shows improvements in the inverse error in the growth index, γ_{FOM} .

vey we assume OPT+SZ with flat external priors on nuisance parameters. We see that clusters make the total principal components look more “cluster-like” (compare to Fig. 1) since they add a lot of information to the total. For the same reason, clusters move the weight of the best-determined PC toward lower redshifts.

The right panel of Fig. 2 shows the accuracies $\sigma(\alpha_i)$ with which the coefficients α_i of the principal components can be measured. The contribution of clusters becomes more pronounced for higher PC number, leading to a nearly constant fractional improvement in error. With clusters, the fourth eigencoeficient is about as well con-

strained as the second eigencoeficient in the baseline case without clusters.

If external priors on the nuisance parameters are available, the full power of cluster constraints is even more evident. To model such priors, we scale all errors by the same fractional value — for each nuisance parameter p_i , we let $F_{ii} \rightarrow F_{ii}(1 + \alpha)$ where α varies from zero (flat prior) to infinity (sharp prior). Consequently, the additional information in each nuisance parameter is a fixed fraction of the original (unmarginalized) error in the parameter. While other choices are possible for adding priors, we settle on this simple prescription to illustrate the

effects of external information on nuisance parameters.

The left panel of Fig. 3 shows the ratio of the figure of merit that includes all probes, FoM, and the FoM with clusters left out (that is, FoM/FoM₀ where FoM₀ = 116). We consider three cluster survey scenarios: an optical survey, an SZ survey with optical follow-up for photometric redshift measurements only¹, and the cross-calibrated OPT+SZ survey. On the x-axis we show the effective prior on the scatter in mass (the quantity $(\sigma_{\ln M}^2(z))^{1/2}$ from Eqs. (2) and (4)) — priors are added to other nuisance parameters as well, we simply do not show them. The plot shows that the OPT+SZ combination improves the total FoM by more than a factor of four if the scatter is known to high precision. In the more realistic cases where mass scatter (and other corresponding parameters) are known to finite accuracy from independent measurements, we still see improvement by factors of ~ 3 .

Priors on nuisance parameters contribute to the information content only if they are substantially stronger than the intrinsic (“self-calibrated”) uncertainties in these parameters; for the scatter in mass, for example, this implies the knowledge of $(\sigma_{\ln M}^2(z))^{1/2}$ to better than $O(1)$ as Fig. 3 shows. Comparing the OPT, SZ, and OPT+SZ cases, we see that as prior information approaches zero (high values of σ_{prior}), the cross-calibration provides a lot of extra information relative to OPT or SZ alone.

The right panel of Fig. 3 shows the corresponding figure of merit for the growth index γ . Even stronger improvements are now seen, with the γ figure of merit increasing between a factor of two (flat priors) and ten (infinitely sharp priors). However, we caution that simulations of modified gravity models need to be done to determine whether the impact of modified structure growth on the cluster abundance is adequately captured by the γ parameter. Nevertheless, the right panel of Fig. 3 indicates that clusters appear to have at least as much potential to improve the pre-JDEM constraints on the growth history of the universe as they do for the expansion history (a similar conclusion has been reached in Ref. [41] for a specific modified gravity model). We also see that the SZ survey is more useful for improving γ FoM than the DETF FoM; this is because SZ probes higher redshifts, which allows for improved constraints on the redshift evolution of the growth of structure and hence γ .

V. DISCUSSION: IMPLICATIONS OF THE ASSUMPTIONS

In this section we discuss the validity of the assumptions we made and the consequences of varying those

assumptions. We divide our assumptions into optimistic and pessimistic.

The assumptions we consider optimistic are:

- The optical mass threshold ($M^{\text{th}} = 10^{13.5} h^{-1} M_{\odot}$);
- The SZ mass threshold ($M^{\text{th}} = 10^{14.2} h^{-1} M_{\odot}$);
- Perfect selection for both SZ and optical cluster finding;
- SPT area (4000 sq. deg.; could be less);
- Known functional form of the scatter in the mass-observable relation (lognormal);
- No mass dependence in the SZ mass-observable scatter (see Eq. (2)).
- Perfect knowledge of photometric redshift errors.

The assumptions that are arguably pessimistic are:

- No other cluster techniques (e.g. X-ray or weak lensing) are available to further cross-calibrate cluster counts;
- Large fiducial value of scatter for both optical ($\sigma_0 = 0.5$) and SZ ($\sigma_0 = 0.25$);
- Area of DES (4,000 sq. deg.; could be as large as 10,000 sq. degrees);
- Low redshift range of optical cluster-finding ($z < 1$);
- Cubic polynomial evolution of redshift scatter for optical and SZ and mass evolution of optical scatter (Lima & Hu, 2005 [20] show that cubic redshift evolution of the scatter yields near-maximal degradation of cosmological parameters);
- Constraints are based on our current knowledge of cluster physics, while the field is developing rapidly.

The first three optimistic assumptions are the most important. Since the mass-function falls rapidly with increasing mass, the lower mass bins contain most of the clusters, and are therefore most relevant. Cunha (2009) [32] shows that cross-calibration decreases the sensitivity of the constraints to the mass threshold somewhat. Here we have checked that increasing the optical limit from $\log M^{\text{th}} = 13.5$ to 13.7, or the SZ limit from 14.2 to 14.5 degrades the figures of merit by 10-20%. Increasing both leads to 30% degradation in the FoMs. The importance of uncertainty in photometric redshift errors has been studied extensively by [21]. For the surveys we consider here, it is not unreasonable to assume that large enough training sets will be available to sufficiently constrain the evolution of the redshift errors and characterize the survey selection.

Of the pessimistic assumptions, the first one is especially significant: for example, if X-ray information is available (as expected from surveys such as eRosita), then X-ray plus optical cross-calibration alone can lead to excellent dark energy constraints even with the unexpected failure of one or more of our SZ assumptions.

To test assumptions about the functional form of the scatter, we added another Gaussian to both optical and

¹ For SPT, optical follow-up is expected from the DES, the Blanco Cosmology Survey (BCS) and the Magellan Telescope.

SZ mass-observable relations², for a total of 27 new parameters (43 total); the new parameters describe the evolution with redshift and mass of the mean and variance of the new Gaussian (cf. Eqs. 3 and 4), the ratio between the two Gaussians describing each mass-observable relation, and the correlation coefficient between optical and SZ (see [32]). The figures of merit degrade by merely 15-20%. The small additional degradation is a consequence of the fact that the new nuisance parameters do not introduce significant new degeneracies with cosmological parameters. If we instead add 4 parameters to characterize the *mass dependence* of the SZ scatter and bias, the degradations are even weaker, being $\lesssim 5\%$. Intuitively, adding mass-dependent evolution of the SZ bias and scatter is not as important as the functional form of the scatter because the SZ probes too narrow a range of masses for the evolution to be significant.

The arguments and tests outlined in this section show that the assumptions made in this paper are not overly optimistic, and that the unforeseen systematic effects would have to be rather capricious in order to lead to significant further degradations in the cosmological constraints.

VI. CONCLUSIONS

We have shown that galaxy clusters are a potentially powerful complement to other probes of dark energy. Assuming optimally combined optical and SZ cluster surveys based on fiducial DES and SPT expectations and allowing for a generous set of systematic errors (a total of 16 nuisance parameters), we have shown that the constraints on the figure of merit expected in 2016 from baryon acoustic oscillations, type Ia supernovae, weak lensing, and Planck improves by nearly a factor of two when clusters are added. This improvement is achieved

without any external prior knowledge on the cluster mass-observable nuisance parameters (but also without explicitly allowing for errors in the theoretically predicted mass function or cluster selection).

We have further illustrated the cluster contribution to constraints by computing, for the first time, the principal components of the equation of state of dark energy for clusters alone and clusters combined with other probes. We found that the first cluster principal component peaks at $z \simeq 0.3$, indicating the “sweet spot” of cluster sensitivity to dark energy. This redshift increases slightly if external information on the cluster nuisance parameters is available. Each eigencoefficient of the principal component expansion is improved by about a factor of two when clusters are added, indicating that the improvements extend to well beyond one or two parameters.

Finally, we have shown that measurements of the growth index of linear perturbations γ (which is a proxy for testing modified gravity) improve by a factor of several with cluster information. While this particular calculation depends on assumptions about the modified gravity model, it broadly illustrates the intrinsic power of clusters to measure growth and distance separately and to obtain useful constraints on modified gravity explanations for the accelerating universe.

We conclude that cross-calibrated cluster counts have enough intrinsic information to significantly improve constraints on dark energy even if the associated systematics are not precisely known.

Acknowledgments

CC and DH are supported by the DOE OJI grant under contract DE-FG02-95ER40899, NSF under contract AST-0807564, and NASA under contract NNX09AC89G. DH thanks the Galileo Galilei Institute in Firenze for good coffee, and we thank an anonymous referee, Gus Evrard and Eduardo Rozo for comments.

-
- [1] J. Frieman, M. Turner, and D. Huterer, *Ann. Rev. Astron. Astrophys.* **46**, 385 (2008).
 - [2] G. Holder, Z. Haiman, and J. J. Mohr, *Astrophys. J. Lett.* **560**, L111 (2001).
 - [3] M. Sahlén, P. T. P. Viana, A. R. Liddle, A. K. Romer, M. Davidson, M. Hosmer, E. Lloyd-Davies, K. Sabirli, C. A. Collins, P. E. Freeman, et al., *Mon. Not. R. Astron. Soc.* **397**, 577 (2009), 0802.4462.
 - [4] G. M. Voit, *Reviews of Modern Physics* **77**, 207 (2005), arXiv:astro-ph/0410173.
 - [5] R. A. Battye and J. Weller, *Phys. Rev. D* **68**, 083506 (2003), arXiv:astro-ph/0305568.
 - [6] P. Rosati, S. Borgani, and C. Norman, *Annu. Rev. Astron. Astrophys.* **40**, 539 (2002), arXiv:astro-ph/0209035.
 - [7] Z. Haiman, J. J. Mohr, and G. P. Holder, *Astrophys. J.* **553**, 545 (2001), arXiv:astro-ph/0002336.
 - [8] L. Marian and G. M. Bernstein, *Phys. Rev. D* **73**, 123525 (2006), arXiv:astro-ph/0605746.
 - [9] E. Pierpaoli, S. Borgani, D. Scott, and M. White, *Mon. Not. R. Astron. Soc.* **342**, 163 (2003), arXiv:astro-ph/0210567.
 - [10] E. Rozo et al. (2009), arXiv:0902.3702.
 - [11] M. D. Gladders, H. K. C. Yee, S. Majumdar, L. F. Barrientos, H. Hoekstra, P. B. Hall, and L. Infante, *Astrophys. J.* **655**, 128 (2007), arXiv:astro-ph/0603588.
 - [12] A. Mantz, S. W. Allen, H. Ebeling, and D. Rapetti, *Mon. Not. R. Astron. Soc.* **387**, 1179 (2008), 0709.4294.
 - [13] A. Vikhlinin et al. (2008), arXiv:0812.2720.
 - [14] J. P. Henry, A. E. Evrard, H. Hoekstra, A. Babul, and A. Mahdavi, *Astrophys. J.* **691**, 1307 (2009), 0809.3832.
 - [15] A. Albrecht, L. Amendola, G. Bernstein, D. Clowe, D. Eisenstein, L. Guzzo, C. Hirata, D. Huterer, R. Kirshner, E. Kolb, et al. (2009), arXiv:0901.0721; <http://jdem.gsfc.nasa.gov/fomswg.html>.
 - [16] J. Ruhl et al., in *Proceedings of the SPIE* (2004), vol. 5498, pp. 11–29.
 - [17] The Dark Energy Survey Collaboration (2005), astro-ph/0510346.

- [18] C. E. Cunha, Phys. Rev. D **79**, 063009 (2009).
- [19] M. Lima and W. Hu, Phys. Rev. D **70**, 043504 (2004).
- [20] M. Lima and W. Hu, Phys. Rev. D **72**, 043006 (2005).
- [21] M. Lima and W. Hu, Phys. Rev. D **76**, 123013 (2007).
- [22] H.-Y. Wu, E. Rozo, and R. H. Wechsler (2008), arXiv:0803.1491.
- [23] P. Predehl et al., in *UV, X-Ray, and Gamma-Ray Space Instrumentation for Astronomy XV. Edited by Siegmund, Oswald H. Proceedings of the SPIE, Volume 6686, pp. 668617-668617-9 (2007)*. (2007), vol. 6686 of *Presented at the Society of Photo-Optical Instrumentation Engineers (SPIE) Conference*.
- [24] R. Giacconi et al. (2009), 0902.4857.
- [25] A. Vikhlinin et al. (2009), 0903.2297.
- [26] L. D. Shaw, G. P. Holder, and P. Bode (2008), arXiv:0803.2706.
- [27] A. V. Kravtsov, A. Vikhlinin, and D. Nagai, Astrophys. J. **650**, 128 (2006).
- [28] E. S. Rykoff, A. E. Evrard, T. A. McKay, M. R. Becker, D. E. Johnston, B. P. Koester, B. Nord, E. Rozo, E. S. Sheldon, R. Stanek, et al., Mon. Not. R. Astron. Soc. **387**, L28 (2008).
- [29] A. E. Evrard, J. Bialek, M. Busha, M. White, S. Habib, K. Heitmann, M. Warren, E. Rasia, G. Tormen, L. Moscardini, et al., Astrophys. J. **672**, 122 (2008).
- [30] E. S. Rykoff, T. A. McKay, M. R. Becker, A. Evrard, D. E. Johnston, B. P. Koester, E. Rozo, E. S. Sheldon, and R. H. Wechsler, Astrophys. J. **675**, 1106 (2008).
- [31] J. D. Cohn, A. E. Evrard, M. White, D. Croton, and E. Ellingson (2007), arXiv:0706.0211.
- [32] C. E. Cunha and A. E. Evrard, ArXiv e-prints (2009), 0908.0526.
- [33] J.-B. Melin, J. G. Bartlett, and J. Delabrouille, Astron. Astrophys. **459**, 341 (2006).
- [34] E. J. Hallman, B. W. O'Shea, J. O. Burns, M. L. Norman, R. Harkness, and R. Wagner, Astrophys. J. **671**, 27 (2007).
- [35] M. R. Becker, T. A. McKay, B. Koester, R. H. Wechsler, E. Rozo, A. Evrard, D. Johnston, E. Sheldon, J. Annis, E. Lau, et al., Astrophys. J. **669**, 905 (2007).
- [36] E. Rozo et al. (2008), arXiv:0809.2794.
- [37] A. J. Albrecht et al. (2006), astro-ph/0609591.
- [38] D. Hutnerer and M. S. Turner, Phys. Rev. **D64**, 123527 (2001).
- [39] E. V. Linder, Phys. Rev. D **72**, 043529 (2005).
- [40] D. Hutnerer and G. Starkman, Phys. Rev. Lett. **90**, 031301 (2003).
- [41] J.-Y. Tang, J. Weller, and A. Zablacki (2006), astro-ph/0609028.
- [42] J. D. Cohn and M. White, Mon. Not. R. Astron. Soc. **393**, 393 (2009), 0809.0308.